energies

MDPI

Article

A Comparative-Analysis-Based Multi-Criteria Assessment of On/Off-Grid-Connected Renewable Energy Systems: A Case Study

Ruben Zieba Falama [1,*], Virgil Dumbrava [2,*], Abdelaziz Salah Saidi [3,4], Etienne Tchoffo Houdji [5], Chokri Ben Salah [6,7] and Serge Yamigno Doka [1]

1 National Advanced School of Mines and Petroleum Industries, University of Maroua, Maroua P.O. Box 46, Cameroon
2 Department of Power Systems, Faculty of Power Engineering, Politehnica University of Bucharest, Splaiul Independentei, no 313, District 6, 060042 Bucharest, Romania
3 Department of Electrical Engineering, King Khalid University, Abha 61411, Saudi Arabia
4 Laboratoire des Systèmes Electriques, Ecole Nationale d'Ingénieurs de Tunis, Université de Tunis El Manar, Tunis 1002, Tunisia
5 Department of Renewable Energy, National Advanced School of Engineering, University of Maroua, Maroua P.O. Box 46, Cameroon
6 LASEE Laboratory, University of Monastir, Monastir 5000, Tunisia
7 ISSAT of Sousse, University of Sousse, Sousse 4003, Tunisia
* Correspondence: rubenziebafalama@gmail.com (R.Z.F.); v_dumbrava@yahoo.com (V.D.)

Abstract: Different configurations of on/off-grid-connected hybrid renewable energy systems (HRESs) are analyzed and compared in the present research study for optimal decision making in Sub-Saharan Africa, facing the problems of electricity deficit. A multi-criteria analysis is performed for this purpose using MATLAB software for simulation. The obtained results show that the levelized cost of energy (LCOE) corresponding to 0% power supply deficit probability (PSDP) is 0.0819 USD/kWh, 0.0925 USD/kWh, 0.3979 USD/kWh, 0.3251 USD/kWh, 0.1754 USD/kWh, 0.1641 USD/kWh, 0.5385 USD/kWh, and 1.4515 USD/kWh, respectively, for the Grid-PV/Wind/Battery, Grid-PV/Battery, Grid-Wind/Battery, Grid-Wind, PV/Wind/Battery, PV/Battery, Wind/Battery, and stand-alone Wind systems. The CO_2 emissions are 14,888.4 $kgCO_2$/year, 16,916.6 $kgCO_2$/year, 13,139.7 $kgCO_2$/year, 6430.4 $kgCO_2$/year, 11,439 $kgCO_2$/year, 14,892.5 $kgCO_2$/year, 10,252.6 $kgCO_2$/year, and 1621.5 $kgCO_2$/year, respectively, for the aforementioned systems. It is found that the Grid-connected PV/Wind/Battery is the most cost-effective system leading to a grid energy cost reduction of 30.89%. Hybridization of different renewable energy sources (RESs) could significantly improve the electricity cost and reduce the CO_2 emissions. However, this improvement and this reduction depend on the used RES and the system configuration. On-grid-connected HRESs are more cost-effective than off-grid-connected HRES. The least polluting energy system is the stand-alone Wind system, which allows a reduction in the grid CO_2 emissions by 93.66%. The sensitivity analysis has proven that the long-term investment, the decrease in the battery cost, and the decrease in the discount rate could lead to the reduction in the LCOE.

Keywords: on/off-grid-connected; HRES; RES; PSDP; LCOE; CO_2 emissions

Citation: Falama, R.Z.; Dumbrava, V.; Saidi, A.S.; Houdji, E.T.; Salah, C.B.; Doka, S.Y. A Comparative -Analysis-Based Multi-Criteria Assessment of On/Off-Grid-Connected Renewable Energy Systems: A Case Study. *Energies* **2023**, *16*, 1540. https://doi.org/10.3390/en16031540

Academic Editor: Silvano Vergura

Received: 25 December 2022
Revised: 11 January 2023
Accepted: 30 January 2023
Published: 3 February 2023

1. Introduction

The intensive use of micro-grids in developing countries, and particularly in Sub-Saharan Africa, is the way to improve electricity access in this part of the world. According to a report, the access to electricity in sub-Saharan Africa has decreased in 2021 [1]. With the growing population, the situation could be worse if nothing is done in the very near future to improve the conditions of access to electricity in Africa. The high electricity cost and the unreliable power supply are the causes of the least electrification of Africa.

Because of the wide availability of friendly environmental natural resources such as sun and wind, micro-grid-based renewable energy appears to be more promising for electricity supply in Africa. Micro-grids can operate in the main-grid-connected mode or be fully autonomous. The solutions to the electricity deficit (in the presence of electricity blackouts) and lack of electricity are proposed in the literature by the implementation of micro-grid systems (hybrids energy systems) either connected to the main grid or not. The decrease in the energy cost could be one of the main solutions to widely spread the electricity access. Vendoti et al. [2] found that the energy cost of a reliable PV/Wind/Biomass/Biogas/FC is 0.214 USD/kWh. Kumara and Saini [3] performed the optimization of an off-grid-connected renewable energy system (RES), showing that the optimal cost of energy (COE) of a reliable Photovoltaic/Biomass/Battery system is 0.21779 USD/kWh. Mala and Saini [4] showed that the feasibility COE for rural and remote-area populations of India ranged from 0.1 USD/kWh to 0.162 USD/kWh, when using off-grid RES for electricity supply. The research investigation on a grid-connected RES conducted by Shakti et al. [5] showed that the COE of the proposed system was 0.104 USD/kWh. The studied system was supposed to reduce grid overload.

The cost of an energy system is proportional to its reliability. Mahmoudi et al. [6] demonstrated that the RES cost increases when its reliability is improved. They showed that the cost of a PV/Wind/Battery increases by 36% when its reliability improves by 5%.

Mohammad et al. [7] demonstrated the economic advantage of the on-grid connected HRES in comparison with off-grid connected HRES. They showed that on-grid connected HRESs could reduce the energy cost of off-grid-connected HRESs by more than 30%. Falama et al. [8] demonstrated that the grid-connected PV/Battery was a promising solution for electricity blackouts and could challenge economically, in the long term, the main grid electricity supply system. Ashtiani et al. [9] showed the importance of the grid-connected RES by comparing an on-grid-connected RES with a stand-alone RES. They demonstrated that the PV/Battery connected to the grid is an economically more profitable and efficient system than a stand-alone PV/Battery by 16.8%.

The integration of RESs into energy systems (ESs) reduces the system's CO_2 emissions. Wei et al. [10] showed that the combination of a PV and diesel system reduces the CO_2 emissions by 56%, in comparison with a diesel-only system. Lin et al. [11] demonstrated that the integration of PVs into the grid significantly reduced the CO_2 emissions.

Several studies [12–18] have been performed in the literature to compare different options of ESs. Zhang et al. [12] studied the following RESs: PV/battery, Wind/Battery, PV/Wind/Battery, PV/Battery/PEMFC, Wind/Battery/PEMFC, and PV/Wind/Battery/PEMFC. The optimization software HOMER was used to design these systems. The outcomes of this study proved that the PV/Wind/Battery/PEMFC system was the best option. Jain and Sawle [13] compareddifferent configurations of standalone and grid-connected HRESs for a remote area, based on an economic analysis. The studied systems included the PV/Wind/Micro-hydro/Grid, the PV/WT/Grid, the WT/Micro-hydro/Grid, the PV/Micro-hydro/Grid, the PV/WT/Micro-hydro/Battery/Diesel, the PV/WT/Battery/DG, the WT/Micro-hydro/Battery/Diesel, and the PV/Micro-hydro/Battery/DG. The PV/WT/Micro-hydro/Grid system was identified as the best economical solution to use in the remote area considered as the study site. Thirunavukkarasu and Sawle [14] performed a study of some HRESs. Different scenarios were considered based on the following components: the Photovoltaic, the Wind Turbine (WT), the Diesel generator, the battery, and the converter. HOMER software was used for simulations. The simulations results based on HOMER identified the PV/WT/Diesel/Battery configuration as the most reliable and economical solution to consider in the studied location. Castillo-Calzadilla et al. [15] compared the standalone PV/Battery with the grid, focusing on fossil fuel generation. The PV/Battery was found as the more cost-effective option than the grid. According to Castillo-Calzadilla et al. [16], the off-grid RES could improve the efficiency rate of energy facilities from 15% to 30%. However, the grid-connected RESs are more advantageous when considering the economic criteria. A comparative analysis of HRESs was performed by Asamoah et al. [17] for water supply in a commu-

nity of Ghana, using HOMER. The studied systems were the Grid-PV and the PV-Genset hybrid systems. The PV/Grid was economically the best option, while the PV-Genset was found as the environmentally best option. Different off-grid HRESs were analyzed and compared for electricity supply in Southern Cameroon by Muh and Tabet [18]. The PV/Diesel/Micro-hydro/Battery configuration was identified as the most economic viable solution for electricity supply in Southern Cameroon.

Various techniques and software [19–23] have been used to optimize energy systems with different performances. The performance of the optimization methods for power systems, based on metaheuristics algorithms, has been demonstrated in various studies [24–29]. The multi-objective Firefly algorithm (MOFA) has been chosen in this work, based on its performance in comparison to some other multi-objective optimization techniques using metaheuristics algorithms [30,31].

This present study focuses on the following research gaps: (1) many HRESs are used for electricity supply, but their strengths and drawbacks are not often clearly presented in Sub-Saharan Africa; (2) the electricity cost reduction is not automatically effective when connecting the HRES to the grid; it could also depend on the used RES and its contribution rate to the whole system energy supply; (3) the choice of the RES for energy supply could also highly influence the reduction rate of the environmental pollution; (4) the optimal decision making on the on/off-grid-connected HRES should be extended to multi-criteria evaluation, not only limited to reliability, economic, and environmental aspects.

Thus, the contribution of this work is to propose some HRESs to overcome the problem of the lack of electricity in Sub-Saharan Africa by considering a case study in Cameroon. The choice of the proposed HRES is based on the potential rate of the available energy resources in the site. Both on- and off-grid-connected HRES are analyzed and compared for optimal decision making. A multi-criteria analysis is performed for this purpose to bring out the strengths and the drawbacks of each energy system proposed. Different rates of the grid contribution to the total system energy supply are considered to study the influences of the HRES penetration rate on the studied systems.

2. Presentation of the Study Systems and Site

2.1. System Configurations and Study Site

Eight different configurations of on/off-grid-connected RESs are studied and compared in the present research work. These energy systems include:

- Grid-PV/Wind/Battery;
- Grid-PV/Battery;
- Grid-Wind/Battery;
- Grid-Wind;
- PV/Wind/Battery;
- PV/Battery;
- Wind/Battery;
- Stand-alone Wind.

Ngaoundéré, which is located in Cameroon, is chosen as the site of study. Figure 1 presents the location of this site. The main representative configuration of the systems to study is presented in Figure 2. The different combinations of the studied systems are given in Table 1. The monthly average daily profile of solar potential is presented in Figure 3. The average monthly wind speed data, irradiation, and ambient temperature of Ngaoundéré are given in Table 2. The monthly average daily profile of ambient temperature of Ngaoundéré is presented in Figure 4.

Figure 1. Location of Ngaoundéré on the geographical map [32].

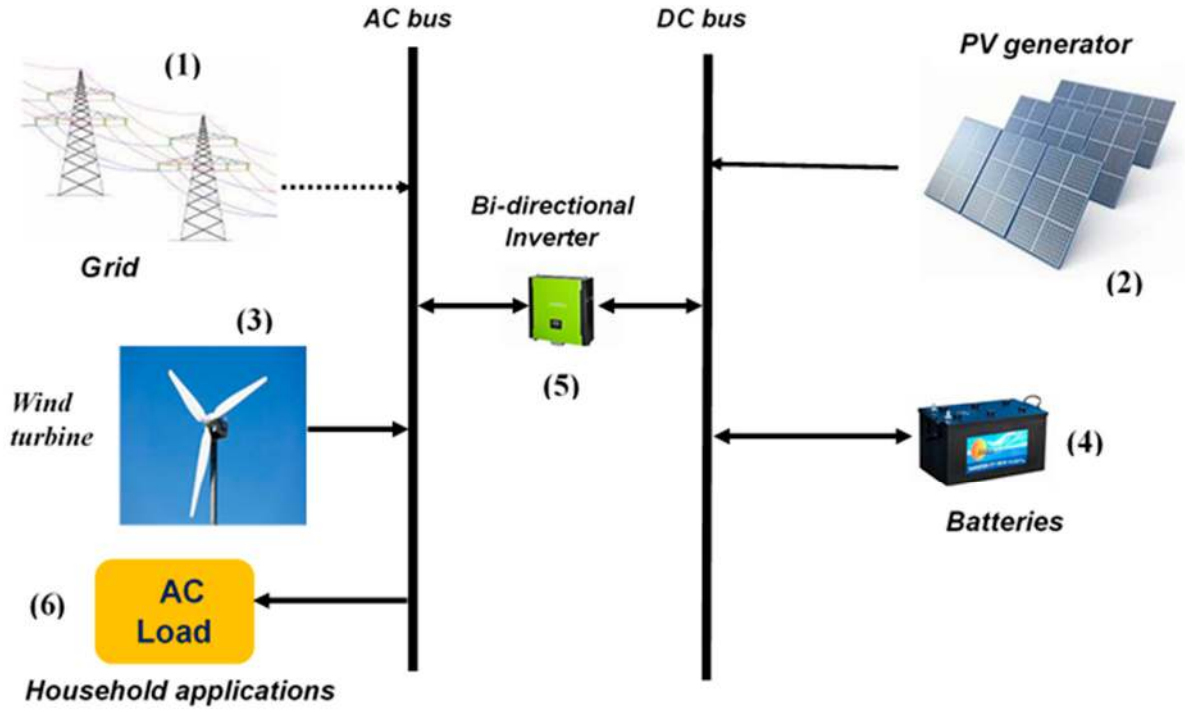

Figure 2. Main configuration of the studied systems.

Table 1. System configurations with their different components.

System Configuration	Components					
Grid-PV/Wind/Battery	Grid	PV generator	Wind turbine	Battery	Bidirectional inverter	Load
Grid-PV/Battery	Grid	PV generator	-	Battery	Bidirectional inverter	Load
Grid-Wind/Battery	Grid	-	Wind turbine	Battery	Bidirectional inverter	Load
Grid-Wind	Grid	-	Wind turbine	-	-	Load
PV/Wind/Battery	-	PV generator	Wind turbine	Battery	Bidirectional inverter	Load
PV/Battery	-	PV generator	-	Battery	Inverter	Load
Wind/Battery	-	-	Wind turbine	Battery	Bidirectional inverter	Load
Wind	-	-	Wind turbine	-	-	Load

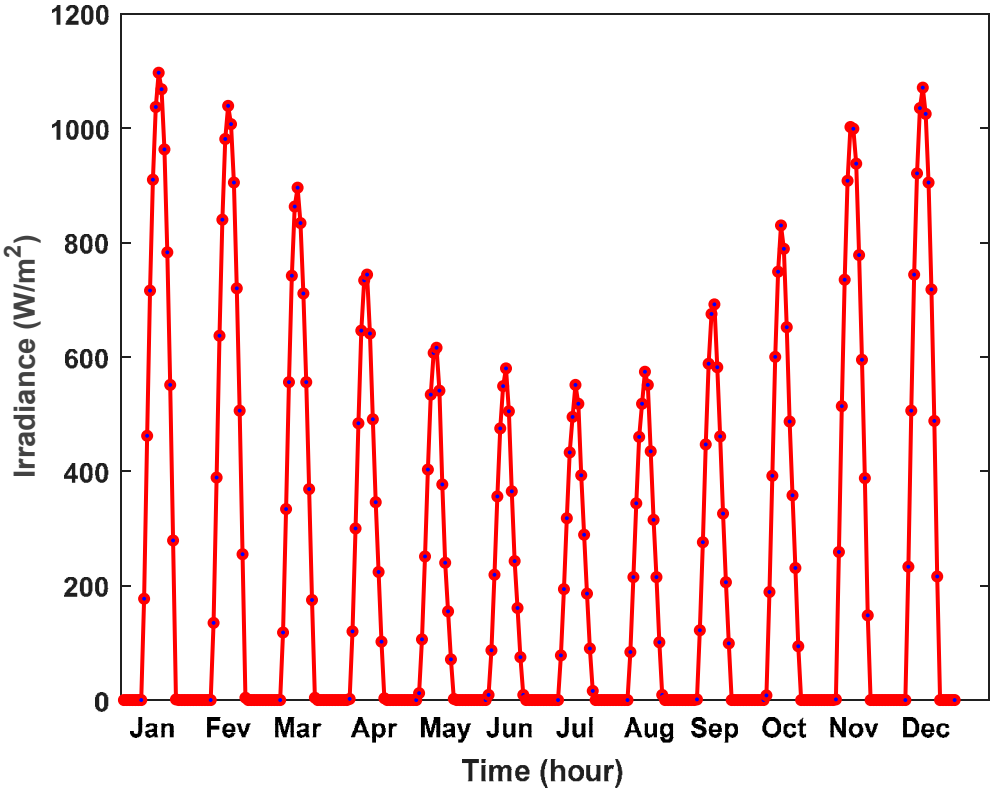

Figure 3. Monthly hourly irradiance data over one year [33].

Table 2. Average monthly data of irradiation, ambient temperature, and wind speed (50 m height) of the study site [33,34].

Month	Wind Speed (m/s)	Irradiation (kWh/m^2)	Ambient Temperature (°C)
Jan.	4.32	7.53	23.4
Feb.	4.35	7.37	25.6
Mar.	4.72	5.83	26.2
Apr.	4.9	6.11	24.5
May	4.59	5.47	22.8
Jun.	3.97	5.06	21.6
Jul.	3.67	4.73	20.9
Aug.	3.56	5.11	20.8
Sept.	3.32	5.02	21.4
Oct.	3.58	5.83	22.7
Nov.	4.01	6.47	24.3
Dec.	4.45	6.31	23.4

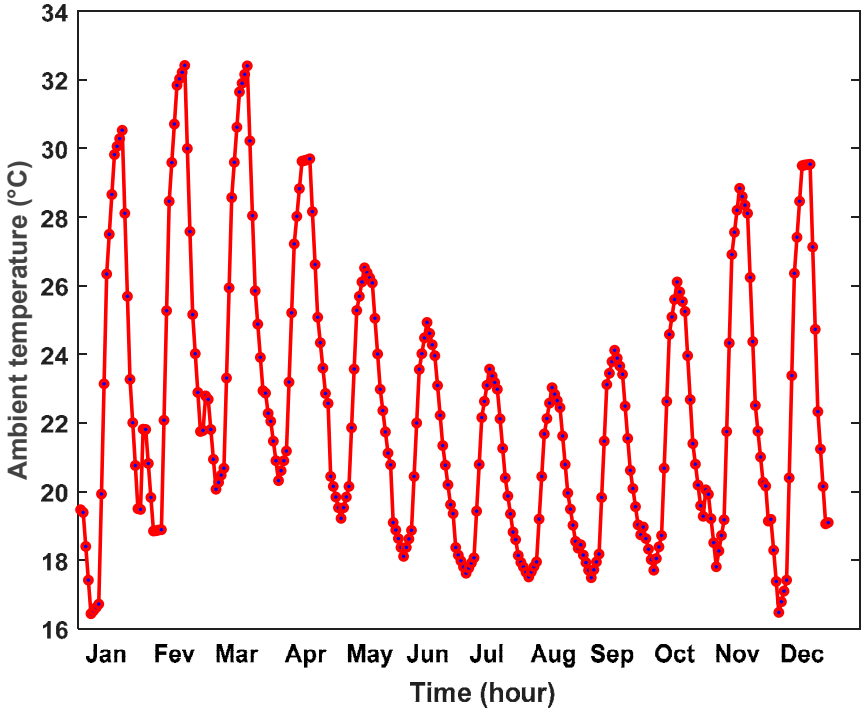

Figure 4. Monthly hourly ambient temperature over the year [33].

2.2. Load Profile

Load demand is essentially for household application. A case study of 70 households in a rural area of Ngaoundéré in Cameroon is considered in the present study. The yearly energy demanded by this population is 38,708 kWh/year. The estimated load profile is presented in Figure 5.

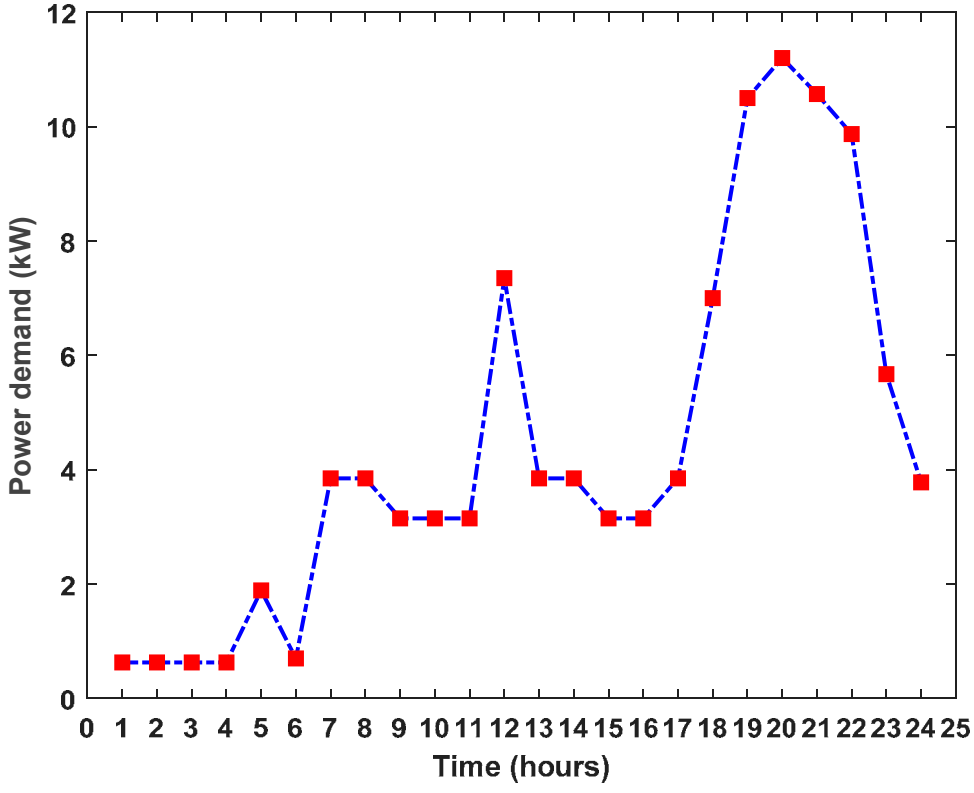

Figure 5. The daily profile of the load demand.

3. Optimization model

3.1. Presentation of the Optimization Algorithm

A powerful tool for the optimization method developed by Yang [35,36], namely the Firefly optimization algorithm (FA), is dedicated to solving optimization problems subjected to some constraints. The Firefly algorithm belongs to the family of metaheuristic bio-inspired algorithms. This algorithm can be applied to find the solutions of multi-objective optimization problems. MOFA is applied in the present study to solve the objective functions containing the technical and economic parameters of the designed systems.

The pseudo-code of a MOFA to solve two objective functions, which is presented in Appendix A of the manuscript (Table A1), has been developed by Yang [36]. This pseudo-code is used in the current research analysis to evaluate the optimal key parameters of the studied ES. The working principle of this algorithm consists of finding the best solutions based on the minimization of the objective functions.

Considering the aforementioned pseudo-code, the updated position of the firefly a is given by the following relationship in Equation (1):

$$\chi_a^{updated} = \chi_a^{initial} + \beta_0 e^{-\gamma \delta_{ab}^2} \left(\chi_b^{initial} - \chi_a^{initial} \right) + \alpha \varepsilon \quad (1)$$

In Equation (2), δ_{ab} is given by:

$$\delta_{ab} = \sqrt{\sum_{k=1}^{N} (\mu_{a,k} - \mu_{b,k})^2} \quad (2)$$

The updated position of firefly a is represented by $\chi_a^{updated}$, while its initial position is represented by $\chi_a^{initial}$. The initial position of firefly b is given by $\chi_b^{initial}$. The distance separating fireflies a and b is symbolized by δ_{ab}. The parameters α, γ, β_0, and ε represent, respectively, the randomization parameter, light absorption coefficient, attractiveness for $\delta_{ab} = 0$, and random value deduced from a gaussian or uniform distributions.

3.2. Grid Modeling

A grid factor is defined to measure the availability of grid energy to respond to the load demand. The maximum energy available from the grid is considered to be equal to the total load demand. The grid factor defines the proportion of grid energy used to meet the load requirement in the ES. When this factor is equal to 1, then all of the energy consumed is ensured by the grid. This factor decreases when the other components of the ES contribute to the load demand. This last case could also correspond to situations where the grid alone is unable to respond effectively to the load demanded. The instantaneous grid power supply is defined by Equation (3):

$$P_G(t) = \varepsilon_G \times P_D(t) \quad (3)$$

where ε_G is the grid factor and P_D is the power demand.

3.3. The PV Modeling

The PV power produced at the time interval t is calculated by Equation (4), while the related PV energy is evaluated through Equation (5).

$$P_{pv}(t) = X_{pv} \cdot P_{Pv,ref} \cdot \left(\frac{G}{G_{ref}} \right) \cdot \left[1 - \alpha \left(T_c - T_{c,ref} \right) \right] \quad (4)$$

$$E_{pv}(t) = P_{Pv}(t) \times \Delta t \times \eta_{inverter} \quad (5)$$

The cell temperature T_c is given by Equation (6):

$$T_c = T_a + \frac{NOCT - 20}{800} \cdot G \quad (6)$$

$P_{pv,ref}$ represents the PV power at MPP in STC, X_{pv} is the multiplication factor of the PV power, $\eta_{inverter}$ is the inverter efficiency, and Δt is the time interval.

3.4. Wind Turbine Modeling

The adjustment of the wind speed for height is used in this study following Equation (7):

$$v_2(y_2) = v_1(y_1) \times \left(\frac{y_2}{y_1}\right)^{\sigma} \tag{7}$$

The law power exponent σ is given by Equation (8) [37]:

$$\sigma = \frac{0.37 - 0.088\ln(v_1)}{1 - 0.088\ln(\frac{y_2}{10})} \tag{8}$$

The wind output energy calculation model is given by the following relationship in Equation (9):

$$P_{WT}(t) = X_{WT} \times P_{R,WT} \times \left[\frac{e^{-(V_{in}/c)^k} - e^{-(V_r/c)^k}}{(V_r/c)^k - (V_{in}/c)^k} - e^{-(V_{off}/c)^k}\right] \tag{9}$$

The shape parameter k is calculated by Equation (10) [38], and the scale parameter c is determined by Equation (12) [39].

$$k = 0.83 \times \overline{V}^{0.5} \tag{10}$$

where

$$\overline{V} = \frac{1}{n}\sum_{i=1}^{n} V_i \tag{11}$$

$$c = \left(\frac{1}{n}\sum_{i=1}^{n}(V_i)^k\right)^k \tag{12}$$

The total annual wind energy produced is given by Equation (13):

$$E_{WT}(t) = P_{WT}(t) \times \Delta t \tag{13}$$

In the above equations, $P_{R,WT}$ represents the wind turbine rate power, X_{WT} is the wind turbine power multiplication factor, n is the number of data points of wind speed, v_1 is the wind speed at hub height y_1, v_2 is the wind speed at height y_2 (measured data), and $\overline{V}$ is the mean of n data points of wind speed.

3.5. Battery Storage Modeling

The nominal capacity of batteries is determined using Equation (14):

$$C_{batt}\ (\text{Wh}) = \frac{X_{batt} \times Maximum\ daily\ load\ energy\ (\text{Wh})}{DOD \times \eta_{batt} \times \eta_{inverter}} \tag{14}$$

The batteries state of charge is updated based on Equation (15):

$$SOC_{batt}(t) = SOC_{batt}(t-1) + \frac{P_{batt\_c}(\text{t}).\Delta t.\eta_{batt\_c}}{C_{batt}} - \frac{P_{batt\_d}(t).\Delta t}{\eta_{batt\_d}.C_{batt}} \tag{15}$$

X_{batt} represents the battery capacity multiplication factor; DOD is the depth of discharge of batteries (%); η_{batt_c} and η_{batt_d} are, respectively, the charge efficiency and the discharge efficiency of the batteries (%); P_{batt_c} and P_{batt_d} are, respectively, the charge power and the discharge power of batteries (kWh); C_{batt} is the nominal capacity of the batteries.

3.6. Inverter Modeling

The power of the inverter is determined by the following relationship in Equation (16):

$$P_{inverter}(\text{kW}) = \frac{Peak\ of\ the\ daily\ power\ demand}{\eta_{inverter}} \tag{16}$$

By referring to Figure 5, the peak of the daily power demand in the case of the present study is 11.2 kW.

3.7. Economic Modeling

The project duration is 25 years. The net present costs of the PV, wind turbine, batteries, and inverter are, respectively, given by Equations (17)–(20).

$$PV_{cost} = X_{pv} \times \left(PV_{inv} + PV_{repl} + \sum_{x=1}^{25} \frac{PV_{O\&M}}{\left(1 + \frac{i'-f}{1+f}\right)^{x-1}} - PV_{salv} \right) \tag{17}$$

$$WT_{cost} = X_{WT} \times \left(WT_{inv} + WT_{repl} + \sum_{x=1}^{25} \frac{WT_{O\&M}}{\left(1 + \frac{i'-f}{1+f}\right)^{x-1}} - WT_{salv} \right) \tag{18}$$

$$Batt_{cost} = X_{batt} \times \left(Batt_{inv} + Batt_{repl} + \sum_{x=1}^{25} \frac{Batt_{O\&M}}{\left(1 + \frac{i'-f}{1+f}\right)^{x-1}} - Batt_{salv} \right) \tag{19}$$

$$Invert_{cost} = \left(Invert_{inv} + Invert_{repl} + \sum_{x=1}^{25} \frac{Invert_{O\&M}}{\left(1 + \frac{i'-f}{1+f}\right)^{x-1}} - Invert_{salv} \right) \tag{20}$$

The salvage values PV_{salv}, WT_{salv}, $Batt_{salv}$, and $Invert_{salv}$ are calculated by Equation (21), where PV, WT, Batt, or Invert could replace "component".

$$Component_{salv} = Component_{repl} \times \left(\frac{Life_{component} - \left(\omega - Life_{component} \times floor\left(\frac{\omega}{Life_{component}}\right)\right)}{Life_{component}} \right) \tag{21}$$

The economic variables f and i' represent, respectively, the rates of the annual inflation and the nominal interest; ω defines how long the project will last (years); $Life_{component}$ is the component lifetime; "*floor*" is a function used to determine the integer part of a number in MATLAB.

3.8. Design of the System

3.8.1. Assessment Functions

Two objectives functions are simultaneously simulated in this study (Equations (22)–(28)). One of the objective functions is used to minimize the *LCOE* (Equation (22)), and the other one (Equation (28)) is used to minimize the Power Supply Deficit Probability (*PSDP*).

$$LCOE\left(\frac{\$}{kWh}\right) = \frac{(PV_{cost} + WT_{cost} + Batt_{cost} + Invert_{cost}) \times CRF + Cost_{grid\_purchased} - Cost_{grid\_sold}}{E_D} \tag{22}$$

The costs of the grid energy purchased and the energy sold to the grid are given, respectively, by Equations (23) and (24).

$$Cost_{grid\_purchased} = Grid_{elect\_cost} \times E_{grid\_purchased} \tag{23}$$

$$Cost_{grid\_sold} = Grid_{elect\_sold} \times E_{grid\_sold} \tag{24}$$

The total annual energy sold to the grid (representing the excess energy) is given by

$$E_{grid\_sold} = E_S - E_D \tag{25}$$

The CRF is calculated using the following relationship:

$$CRF = \frac{i(1+i)^{\gamma}}{(1+i)^{\gamma} - 1} \tag{26}$$

where

$$i = \frac{i' - f}{1+f} \tag{27}$$

In the above equations, $E_{grid\_purchased}$ is the total annual grid energy purchased; $Grid_{elect\_cost}$ represents the price of electricity in Cameroon; $Grid_{elect\_sold}$ is the electricity cost sold to the grid, which represents 50% of the national grid electricity cost purchased [40]; i is an economic parameter called interest rate.

The power supply deficit probability ($PSDP$) is defined by:

$$PSDP(\%) = \frac{\sum_{t=1}^{8760} hours\left[P_{supply}(t) < P_{demand}(t)\right]}{8760} \tag{28}$$

The parameter values used for simulation, related to the studied systems, are presented in Table 3.

Table 3. Parameter specifications used for simulation.

Designation	Value
PV specifications	
PV module	SEP 290W/295W/300W HC [41]
PV rated power	300 W
Initial investment	1500 USD/kW [42]
Replacement	1500 USD/kW
O and M	1% of investment/year [43]
Component lifetime (years)	25
CO_2 emissions	40 gCO_2/kWh [44]
Wind turbine specifications	
Type	Raum Energy 3.5 [45]
Rated power	3.5 kW
Hub height	14.5 m
Rated wind speed	16 m/s
Cut-in wind speed	4 m/s
Cut-off wind speed	25 m/s

Table 3. *Cont.*

Designation	Value
Initial investment	3000 USD/kW [46]
Replacement	3000 USD/kW
O and M	3% of investment/year [46]
Component lifetime (years)	20
CO_2 emissions	11 g/kWh [21]
Battery specifications	
Efficiencies of charge and discharge	85%
DOD	80%
Minimum SOC	20%
Initial investment	0.213 USD/Wh [46]
Replacement	0.213 USD/Wh
O and M	3% of investment/year [46]
Component lifetime (years)	25
CO_2 emissions	55.3 $kgCO_2$/kWh [47]
Inverter (or Rectifier) specifications	
Efficiency	95% [4]
Inverter utilization factor	1
Initial investment	715 USD/kW [42,43]
Replacement	715 USD/kW
O and M	100 USD/year [48]
Component lifetime (year)	15
Grid specifications	
CO_2 emissions	660.63 g/kWh [7,49,50]
Financial specifications	
Nominal interest rate	8%
Value of annual inflation rate	4%
Project lifetime	25 years

3.8.2. Optimization Constraints and Operational Strategy

The constraints leading to the optimal design of the ES studied are given by Equations (29)–(32).

$$P_{pv}(t) + P_{WT} + P_G + P_{batt\_d}(\Delta t) \geq P_D(\Delta t) \quad (29)$$

$$X_{pv,min} \leq X_{pv} \leq X_{pv,max} \quad (30)$$

$$X_{WT,min} \leq X_{WT} \leq X_{WT,max} \quad (31)$$

$$X_{batt,min} \leq X_{batt} \leq X_{batt,max} \quad (32)$$

The operational strategy of the studied systems is described in Figure 6. The power generated P_{gen} combines PV power (P_{pv}), WT power (P_{WT}), and grid power (P_G). For off-grid connected systems, P_G = 0. The PV, wind turbine, and grid powers are given for each Δt = 1 h. Two main situations are highlighted in the presented operational strategy:

(1) If the total generated power P_{gen} fulfills the power demanded with a surplus power ($P_{gen}(t) > P_{demand}(t)$), then the batteries are in charging mode. This charging mode mutates to another one when the state of charge (SOC) of the batteries takes the value 1 and above; in that case, the surplus power is either sold to the grid (for on-grid RES) or lost (for off-grid RES). The SOC is updated using Equation (15).

(2) If the generated power is unable to respond to the load requirement ($P_{gen}(t) < P_{demand}(t)$), then the batteries move to the discharging mode to cover the deficit power ($P_{batt\_d}(t) = P_{demand}(t) - P_{gen}(t)$). However, the batteries are able to provide energy only when the SOC is higher than 20%.

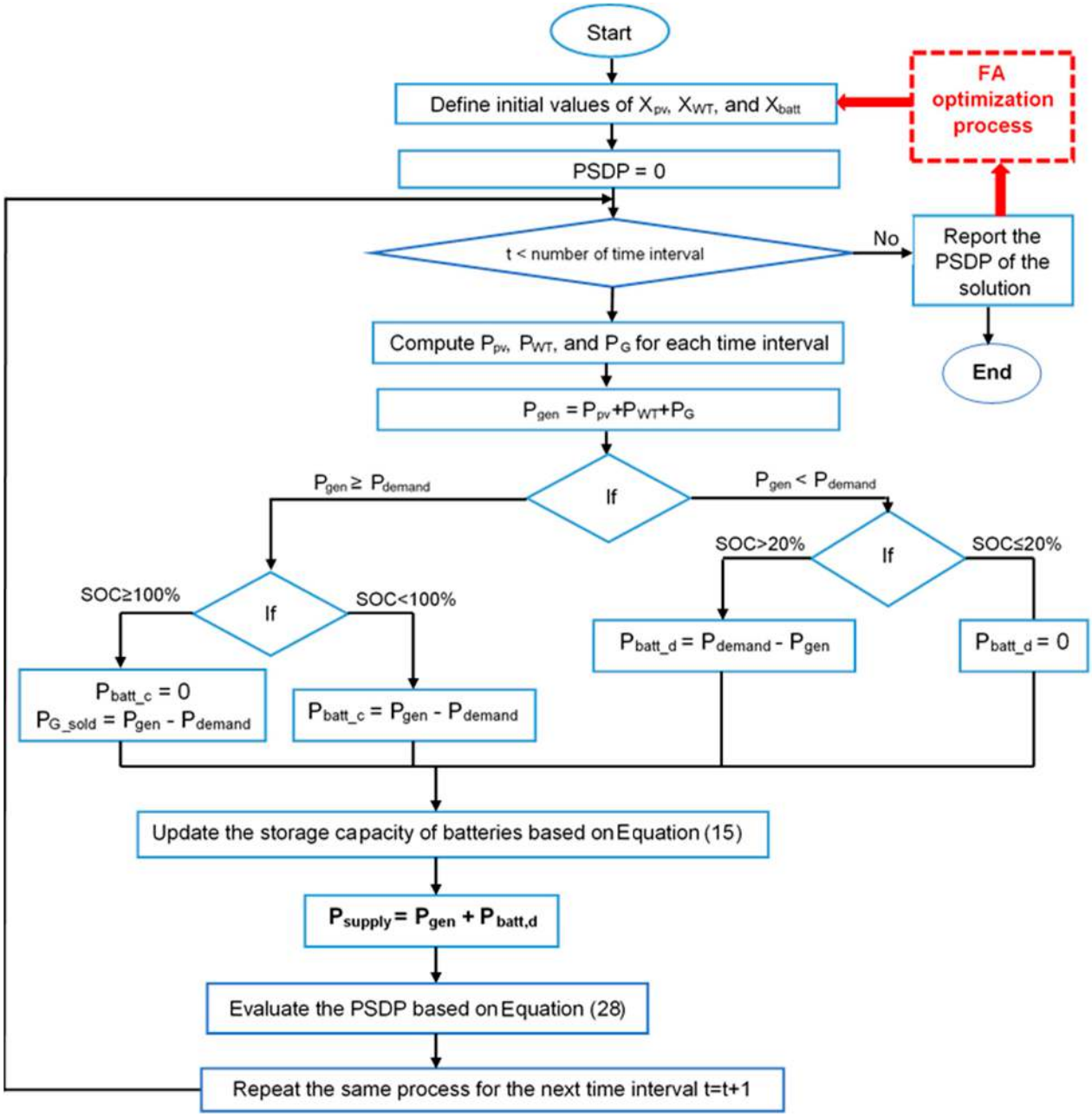

Figure 6. Operational strategy.

4. Results and Discussion

Different options of electricity supply are studied and compared in this research paper considering a case study in sub-Saharan Africa, where the national grid electricity is unable to fully satisfy the load requirement for households' applications. For this purpose, some on- and off-grid-connected RESs are optimally designed and analyzed for decision making. MOFA is performed for the optimal size of the studied systems. The functions defined in Equations (22) and (28) are simulated simultaneously by respecting the optimization constraints defined by Equations (29)–(32) and referring to the operational strategy described in Figure 6. The optimal design configuration for each system considered is identified at the same time by its lowest cost and its best reliability (when PSDP is 0%). The total load requirement is 38,708 kWh/year. A different grid factor is considered for simulation and analysis. The grid electricity cost in Cameroon for an average household consumption is 0.1185 USD/kWh.

The results of Table 4 are obtained for a grid, supplying 20% of the load demand. The characteristics of the designed ES based on techno-economic criteria are presented in this table. These characteristics are obtained for a 0% PSDP. The PV rated power sizes are 24 kW, 22.5 kW, 27.3 kW, and 27.9 kW, respectively, for Grid-PV/Wind/Battery, Grid-PV/Battery, PV/Wind/Battery, and PV/Battery systems. The Wind turbine rated power sizes are 3.5 kW, 59.5 kW, 196 kW, 7 kW, 73.5 kW, and 241.5 kW, respectively, for Grid-PV/Wind/Battery, Grid-Wind/Battery, Grid-Wind, Wind/Battery, and stand-alone Wind systems. The battery nominal capacity sizes are 118.6086 kWh, 195.0434 kWh, 115.8342 kWh, 164.1641 kWh, 312.6341 kWh, and 189.7121 kWh, respectively, for Grid-PV/Wind/Battery, Grid-PV/Battery, Grid-Wind/Battery, PV/Wind/Battery, PV/Battery, and Wind/Battery systems. The inverter power size is 11.8 kW for all the studied systems considered. It is found that the PV and the WT capacities decrease with the increase in the number of the connected energy sources. An on/off-grid-connected PV/Battery requests a higher battery capacity than an on/off-grid-connected Wind/Battery system. This can be explained by the fact that wind turbine generators unlike the PV generator can operate during the night.

Table 4. Optimal characteristics of the systems components.

Scenario	*PSDP* (%)	X_{PV}	X_{WT}	X_{batt}	*PV Capacity* (kW)	*WT Capacity* (kW)	*Battery Capacity* (kWh)	*Inverter Power* (kW)
Grid-PV/Wind/Battery	0	80	1	0.85	24	3.5	118.6086	11.8
Grid-PV/Battery	0	75	-	1.09	22.5	-	195.0434	11.8
Grid-Wind/Battery	0	-	17	0.84	-	59.5	115.8342	11.8
Grid-Wind	0	-	56	-	-	196	-	11.8
PV/Wind/Battery	0	91	2	1	27.3	7	164.1641	11.8
PV/Battery	0	93	-	1.38	27.9	-	312.6341	11.8
Wind/Battery	0	-	21	1.075	-	73.5	189.7121	11.8
Wind	0	-	69	-	-	241.5	-	11.8

It is observed from Figure 7 that the energy supply is higher than the energy demand for the period considered. Thus, the energy provided fully satisfies the load demand and demonstrates the technical qualification of the ES designed.

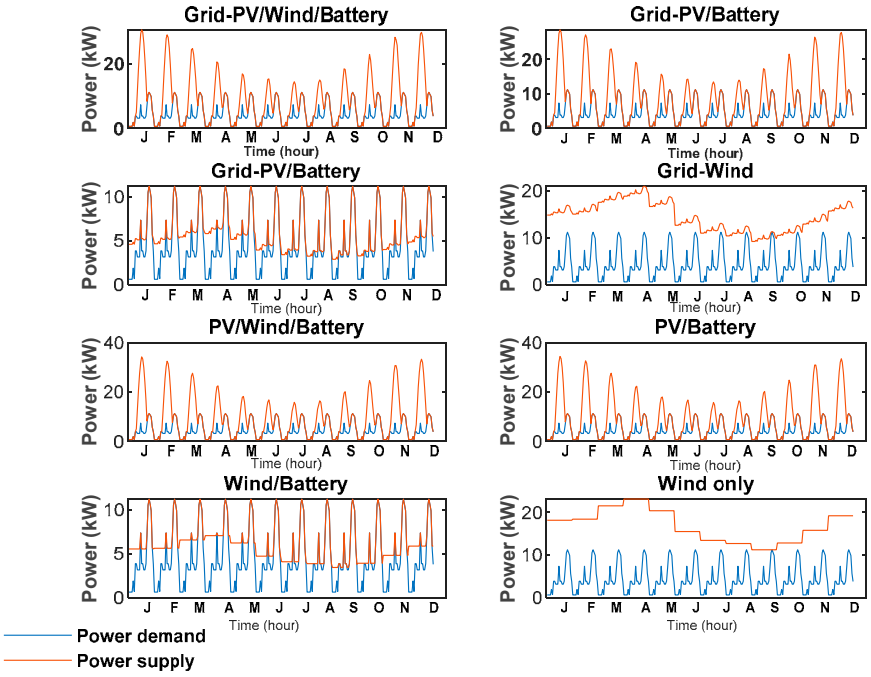

Figure 7. Comparison of the variation in the energy supply and the energy demand over one year period corresponding to 0% *PSDP*.

Table 5 presents the annual energy balance corresponding to the optimal system size in Table 4. It can be seen from Table 6 that the contributions of the PV energy source to the total energy supply generated are 83.73%, 86.03%, 93.12%, and 100%, respectively, for Grid-PV/Wind/Battery, Grid-PV/Battery, PV/Wind/Battery, and PV/Battery systems. The contributions of the Wind energy source to the total energy supply generated are 3.52%, 82.43%, 93.92%, 6.88%, 100%, and 100%, respectively, for Grid-PV/Wind/Battery, Grid-Wind/Battery, Grid-Wind, PV/Wind/Battery, Wind/Battery, and stand-alone Wind energy systems. The contribution of the grid to the total energy supply is 12.75% for the Grid-PV/Wind/Battery system, 13.97% for the Grid-PV/Battery system, 17.57% for the Grid-Wind/Battery system, and 6.08% for the Grid-Wind system. The obtained results show that for an optimal design of on/off-grid-connected renewable energy systems including PV and Wind sources, most of the energy supply generated is provided by the PV source.

Table 5. Annual energy balance corresponding to the optimal characteristic of the studied systems.

Scenario	E_{PV} (kWh)	E_{WT} (kWh)	E_G (kWh)	E_s (kWh)	E_{s_cons} (kWh)	$E_{surplus}$ (kWh)	E_B (kWh)	E_{excess} (kWh)
Grid-PV/Wind/Battery	50,850	2136.3	7741.7	60,728	21,324	39,404	17,384	22,019
Grid-PV/Battery	47,671.3	-	7741.7	55,413	19,948	35,465	18,760	16,705
Grid-Wind/Battery	-	36,318	7741.7	44,060	31,013	13,047	7695.3	5351.5
Grid-Wind	-	119,640	7741.7	127,381.7	38,708	88,670	-	88,670
PV/Wind/Battery	57,841.3	4272.7	-	62,114	17,779	44,335	20,929	23,406
PV/Battery	59,113	-	-	59,113	15,245	43,868	23,464	20,404
Wind/Battery	-	44,864	-	44,864	28,938	15,925.6	9770.3	6155.3
Wind	-	147,410	-	147,410	38,708	108,700	-	108,700

Table 6. Contribution of the different systems' energy sources to the optimal energy supply.

Scenario	E_{PV}/E_s (%)	E_{WT}/E_s (%)	E_G/E_s (%)
Grid-PV/Wind/Battery	83.73	3.52	12.75
Grid-PV/Battery	86.03	-	13.97
Grid-Wind/Battery	-	82.43	17.57
Grid-Wind	-	93.92	6.08
PV/Wind/Battery	93.12	6.88	-
PV/Battery	100	-	-
Wind/Battery	-	100	-
Wind	-	100	-

The total energy supply is distributed in three different ways: the load directly uses one part of this energy, another part is provided to the battery to be re-used, and the rest is sold to the grid (for on-grid-connected RES) or lost (for off-grid-connected RES). It is shown in Table 7 that the surplus energy is less than the load energy consumed ($E_{s\_cons} + E_B$) for all the ES considered, except for Grid-Wind and Wind only. For Grid-Wind and stand-alone Wind, the excess energy represents, respectively, 69.61% and 73.74% of the total energy supply generated. Thus, a high excess energy rate is recorded for an energy system without a storage device and with only one renewable energy source such as wind.

Table 7. Energy supply distribution.

Scenario	E_{s_cons}/E_s (%)	E_B/E_s (%)	E_{excess}/E_s (%)
Grid-PV/Wind/Battery	35.11	28.63	36.26
Grid-PV/Battery	36	33.85	30.15
Grid-Wind/Battery	70.38	17.47	12.15
Grid-Wind	30.39	-	69.61
PV/Wind/Battery	28.63	33.69	37.68
PV/Battery	25.79	39.69	34.52
Wind/Battery	64.50	21.78	13.72
Wind	26.26	-	73.74

The contribution rate of the different components to the load consumption is presented in Table 8. For a grid-connected system including the PV, Wind, and Battery, most of the energy is directly consumed from the main sources (the contribution rate ranges from 51.54% to 100%), and the rest is consumed from the battery (the rate contribution ranges from 19.88% to 48.46%). However, the situation is different when the components are off-grid-connected, particularly for the PV/Wind/Battery and PV/Battery systems, where most of the energy consumed is not directly from the main energy sources but from the battery (54.07% and 60.62% of the energy consumed is from the battery, respectively, for PV/Wind/Battery and PV/Battery). For a Wind-only energy generation source such as in Wind/Battery and stand-alone Wind, most of the energy demanded is supplied by the main energy sources.

Table 8. Contribution rate to the load energy consumed.

Scenario	E_D (kWh)	E_{s_cons}/E_D (%)	E_B/E_D (%)
Grid-PV/Wind/Battery	38,708	55.09	44.91
Grid-PV/Battery	38,708	51.54	48.46
Grid-Wind/Battery	38,708	80.12	19.88
Grid-Wind	38,708	100	-
PV/Wind/Battery	38,708	45.93	54.07
PV/Battery	38,708	39.38	60.62
Wind/Battery	38,708	74.76	25.24
Wind	38,708	100	-

The economic balance is given in Tables 9 and 10. It is found that the battery is the most costly component in Grid-PV/Wind/Battery, Grid-PV/Battery, PV/Wind/Battery, and PV/Battery systems. The contribution of the battery to the total NPC of the HRES represents 47.43%, 62.74%, 44.09%, and 65.04%, respectively, in the aforementioned systems. However, the battery cost represents only 14.85% and 15.43% of the ES net present cost in comparison to the Wind turbine cost, which represents 80.66% and 80.72%, respectively, in Grid-Wind/Battery and Wind/Battery systems. Thus, when the PV is the most important energy supply in an HRES, the system cost is dominated by the battery cost. The main part of the system's cost is attributed to the WT when a great part of the energy generated by the HRES comes from this component.

Table 9. Economic balance of the studied systems.

Scenario	$Cost_{PV}$ (USD)	$Cost_{WT}$ (USD)	$Cost_{Batt}$ (USD)	$Cost_{Inverter}$ (USD)	*Renew NPC* (USD)	*Total LCOE* (USD/kWh)
Grid-PV/Wind/Battery	19,950	12,755	40,395	12,064	85,164	0.0819
Grid-PV/Battery	18,703	-	51,801	12,064	82,568	0.0925
Grid-Wind/Battery	-	216,840	39,920	12,064	268,824	0.3979
Grid-Wind	-	714,300	-	12,064	726,364	0.3251
PV/Wind/Battery	22,693	25,511	47,523	12,064	107,791	0.1754
PV/Battery	23,192	-	65,582	12,064	100,838	0.1641
Wind/Battery	-	267,860	51,088	12,064	331,012	0.5385
Wind	-	880,120	-	12,064	885,670	1.4515

Table 10. Distribution of the net present cost between the components of the systems.

Scenario	$Cost_{PV}/NPC$ (%)	$Cost_{WT}/NPC$ (%)	$Cost_{Batt}/NPC$ (%)	$Cost_{Inverter}/NPC$ (%)
Grid-PV/Wind/Battery	23.43	14.98	47.43	14.17
Grid-PV/Battery	22.65	-	62.74	14.61
Grid-Wind/Battery	-	80.66	14.85	4.79
Grid-Wind	-	98.34	-	1.66
PV/Wind/Battery	21.05	23.67	44.09	11.19
PV/Battery	23	-	65.04	11.96
Wind/Battery	-	80.92	15.43	3.64
Wind	-	98.65	-	1.35

The economic comparison of the different energy systems studied, presented in Figure 8, shows that Grid-PV/Wind/Battery (LCOE = 0.0819 USD/kWh) is the most cost-effective system, followed by Grid-PV/Battery (LCOE = 0.0925 USD/kWh), PV/Battery (LCOE = 0.1641 USD/kWh), PV/Wind/Battery (LCOE = 0.1754 USD/kWh), Grid-Wind (LCOE = 0.3251 USD/kWh), Grid-Wind/Battery (LCOE = 0.3979 USD/kWh), Wind/Battery (LCOE = 0.5385 USD/kWh), and stand-alone Wind (LCOE = 1.4515 USD/kWh). These results demonstrate that the off-grid-connected HRES and the grid-only system could be economically improved by connecting the HRES to the grid. The optimal integration of a PV in a Wind/Battery system leads to the reduction in the system energy cost. However, the optimal addition of a WT to a PV/Battery system leads to an increase in the system's energy cost.

The environmental analysis of the ES studied, described in Table 11 and in Figure 9, shows that the least polluting system is the stand-alone Wind system (1621.5 $kgCO_2$/year), followed by the Grid-Wind system (6430.4 $kgCO_2$/year), the Wind/Battery system (10,252.6 $kgCO_2$/year), the PV/Wind/Battery system (11,439 $kgCO_2$/year), the Grid-Wind/Battery system (13,139.7 $kgCO_2$/year), the Grid-PV/Wind/Battery system (14,888.4 $kgCO_2$/year), the PV/Battery system (14,892.5 $kgCO_2$/year), and the Grid-PV/Battery system (16,916.6 $kgCO_2$/year). The obtained results show that the most polluting components are the battery and grid.

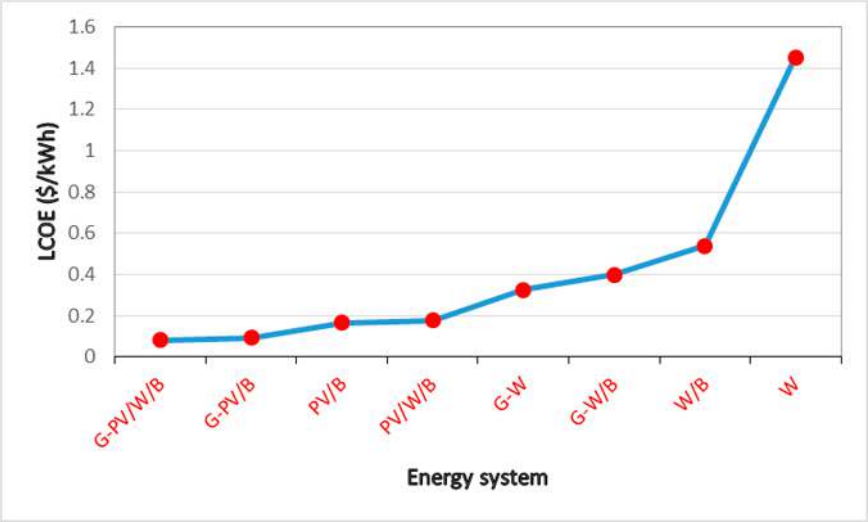

Figure 8. Comparison of the studied systems focusing on their electricity cost.

Table 11. Comparison of the studied systems based on their CO_2 emissions.

Scenario	*PV* ($kgCO_2/y$)	*WT* ($kgCO_2/y$)	*Battery* ($kgCO_2/y$)	*Grid* ($kgCO_2/y$)	*Total* ($kgCO_2/y$)
Grid-PV/Wind/Battery	2034	23.5	7716.5	5114.4	14,888.4
Grid-PV/Battery	1906.9	-	9895.3	5114.4	16,916.6
Grid-Wind/Battery	-	399.5	7625.8	5114.4	13,139.7
Grid-Wind	-	1316	-	5114.4	6430.4
PV/Wind/Battery	2313.7	47	9078.3	-	11,439
PV/Battery	2364.5	-	12,528	-	14,892.5
Wind/Battery	-	493.5	9759.1	-	10,252.6
Wind	-	1621.5	-	-	1621.5

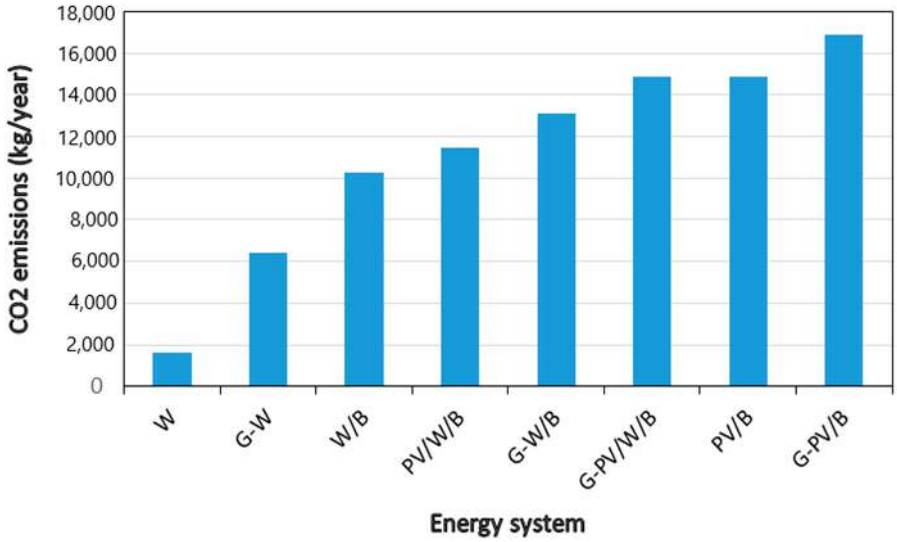

Figure 9. CO_2 emissions from the different studied systems.

Table 12 presents the behavior of the studied grid-connected renewable energy systems submitted to different renewable energy penetration rates (different grid factor availability). It is found that the size of the studied system components decreases when the grid availability factor increases from 0.2 to 1 (renewable energy penetration rate decreases from 80%

to 0% in that case). A grid availability factor equal to 1 means no (or zero) renewable energy penetration. The results of Table 12 show that a higher penetration rate of wind energy (lower grid energy availability factor) corresponds to a higher LCOE. This is demonstrated with the Grid-Wind/Battery and the Grid-Wind systems, where the LCOE increases when the Wind energy penetration rate increases too (the grid factor decreases in that case). However, as shown in Table 12 with the Grid/PV/Battery system, the higher contribution of the PV (the lower grid availability factor) corresponds to the lower LCOE. It is demonstrated that the increase in the PV energy penetration rate (the decrease in the grid availability factor) induces a decrease in the LCOE. For the Grid-PV/Wind/Battery system, the LCOE reduction occurs only for a high renewable energy penetration rate. It is demonstrated in Table 12 that the minimum value for the renewable energy penetration rate (including both PV and Wind energies) to lead to the grid cost reduction is 60% (corresponding to the grid availability factor of 0.4). This limit or critical value is defined by the cumulative influence on the grid cost of the renewable energy sources considered. The influence of the PV energy (leading to cost reduction) and the influence of the Wind energy (leading to cost increasing) are opposite in the present case. Therefore, not all the on-grid-connected HRESs could lead to cost reduction. It depends on the RES used. The connection of PVs to the grid could significantly improve the energy cost.

Table 12. Grid-connected RES submitted to variable grid energy contribution.

Scenario	*Grid Factor*	*LCOE*	X_{PV}	X_{WT}	X_{batt}	*PV Capacity* (kW)	*WT Capacity* (kW)	*Battery Capacity* (kWh)	*Inverter Power* (kW)
Grid-PV/Wind/Battery	0.2	0.0819	80	1	0.85	24	3.5	118.6086	11.8
	0.4	0.1081	53	1	0.69	15.9	3.5	113.2732	11.8
	0.6	0.1262	33	1	0.49	9.9	3.5	80.4404	11.8
	0.8	0.1241	18	1	0.12	5.4	3.5	19.6997	11.8
	1	0.1185	-	-	-	-	-	-	-
Grid-PV/Battery	0.2	0.0925	75	-	1.09	22.5	-	195.0434	11.8
	0.4	0.0996	57	-	0.812	17.1	-	108.2406	11.8
	0.6	0.1106	38	-	0.55	11.4	-	49.6596	11.8
	0.8	0.1188	21	-	0.28	6.3	-	12.8705	11.8
	1	0.1185	-	-	-	-	-	-	-
Grid-Wind/Battery	0.2	0.3979	-	17	0.84	-	59.5	115.8342	11.8
	0.4	0.3367	-	13	0.6	-	45.5	59.0991	11.8
	0.6	0.3035	-	8	0.8	-	28	105.0650	11.8
	0.8	0.2058	-	5	0.1	-	17.5	1.6416	11.8
	1	0.1185	-	-	-	-	-	-	-
Grid-Wind	0.2	0.3251	-	56	-	-	196	-	11.8
	0.4	0.3079	-	42	-	-	147	-	11.8
	0.6	0.2815	-	28	-	-	98	-	11.8
	0.8	0.2359	-	14	-	-	49	-	11.8
	1	0.1185	-	-	-	-	-	-	-

Table 13 presents the impact of the RE penetration rate on the CO_2 emissions of the grid-connected studied energy systems. It is shown that the carbon dioxide emissions decrease when the renewable energy penetration rate increases. When only the grid is able to fully satisfy the load demand, its CO_2 emissions is 25,572 $kgCO_2$/year in the present case. Thus, a grid-connected HRES significantly reduces the CO_2 emissions of the grid.

Table 13. Influence of the renewable energy penetration rate on the system's carbon dioxide emissions.

Scenario	*Grid Factor*	*Renewable Energy Penetration* (%)	*CO_2 Emissions* ($kgCO_2$/Year)
Grid-PV/Wind/Battery	0.2	80	14,888.4
	0.4	60	17,864
	0.6	40	20,654
	0.8	20	22,028
	1	0	25,572
Grid-PV/Battery	0.2	80	16,916.6
	0.4	60	19,050
	0.6	40	21,302
	0.8	20	23,533
	1	0	25,572
Grid-Wind/Battery	0.2	80	13,139.7
	0.4	60	15,981
	0.6	40	22,794
	0.8	20	21,483
	1	0	25,572
Grid-Wind	0.2	80	6430.4
	0.4	60	11,216
	0.6	40	16,001
	0.8	20	20,786
	1	0	25,572

The sensitivity analysis of the studied systems is performed. Indeed, the variation in some parameters of a system could have an influence on its cost. The influences of varying the project lifetime, battery cost, and discount rate on the LCOE are, respectively, presented in Figures 10–12. The values of the parameters given in Table 4 are considered as the base values (or reference values), corresponding to a 100% variation (no variation in the parameters considered). The optimal characteristics of the system components given in Table 5 are obtained for these base values. The corresponding LCOEs are those given in Table 10. It can be observed from Figure 10 that the LCOE of all the studied systems decreases when the project lifetime varies from 20% (5 years) to 180% (45 years). Thus, a long project lifetime is advantageous for the reduction in the LCOE of systems. As shown in Figure 11, the increase in the LCOE of the studied systems is proportional to the variation in the battery cost from 20% to 180%, excluding the systems that are free of battery energy storage (such as Grid-Wind and Wind-only systems for which the variation in the battery cost does not have any influence on their LCOE). Thus, the reduction in the battery cost could improve the LCOE of the studied systems-based battery. It is observed from Figure 11 that the Grid-PV/Battery is economically more advantageous than the Grid-PV/Wind/Battery, for the variation in the battery cost from 20% to 30% (corresponding to the battery reduction cost of 70% to 80%). Likewise, PV/Wind/Battery is more cost-effective than PV/Battery, for the variation in the battery cost from 100% to 180% (corresponding to the battery increasing cost of 40% to 80%). Thus, the importance of the influence of the battery cost differs from one system to another. Figure 12 shows that the LCOE varies increasingly from 20% to 180% of the discount rate variation. Thus, the reduction in this parameter is an asset for the improvement of the LCOE. It can be observed from Figures 10–12 that the parameters that highly influence the LCOE are the project lifetime and the discount rate.

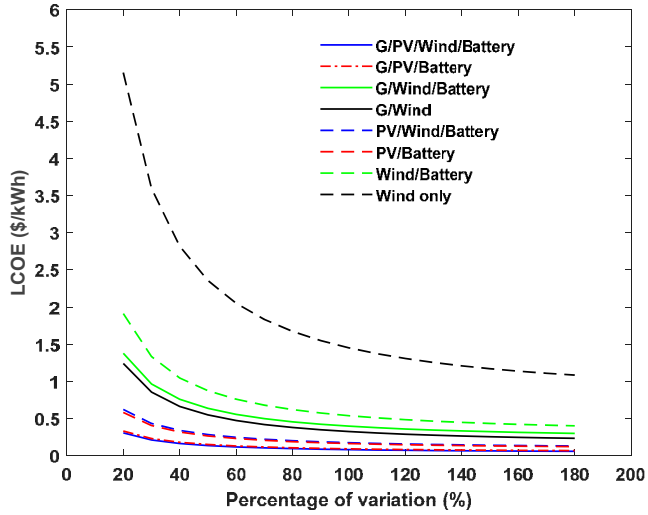

Figure 10. Influence of the variation in the project lifetime on the LCOE of the studied systems.

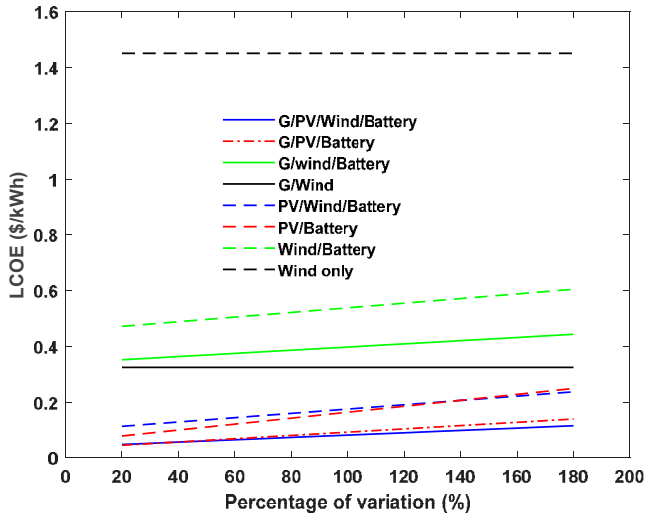

Figure 11. Influence of the variation in the battery cost on the LCOE of the studied systems.

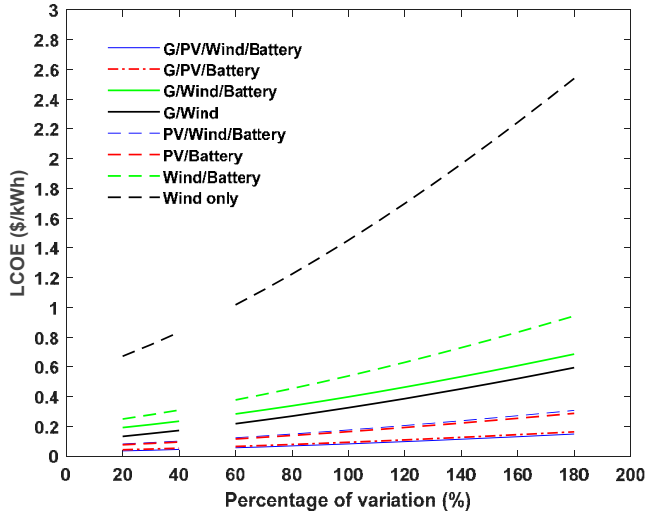

Figure 12. Influence of the variation in the discount rate on the LCOE of the studied systems.

Table 14 summarizes the evaluation and comparative criteria of the different studied systems, leading to optimal decision making. The calculated values are given for a fully

loaded energy supply (perfect reliability). When considering the economic criteria, the Grid-PV/Wind/Battery is the most economically profitable system, leading to the best grid energy cost reduction by 30.89%. Focusing on the environmental consideration, the Wind-only system is the best choice, allowing a grid CO_2 emissions reduction by 93.66%. There are no energy losses for the on-grid-connected HRES, as all the excess energy produced by the HRES is sold to the grid. Based on this, the on-grid-connected HRES is more advantageous than the off-grid-connected HRES. The HRES either connected to the grid or not, having the PV as the main renewable energy source, could lead to significant cost reduction. This situation could not be applied if the main renewable energy source is Wind. However, when Wind is the main RES, the lowest values of CO_2 emissions of the systems are recorded. The main PV system requests a higher energy storage capacity than the main Wind energy system. Thus, the alternative option for energy storage, less expensive than the battery, could be a solution to the significant electricity cost reduction of energy-systems-based HRESs, particularly when the main energy source is the PV.

Table 14. Summary of the different evaluation and comparative criteria of the studied systems for $\varepsilon_G = 0.2$.

Scenario	*Reliability* (%)	*Energy Cost* (USD/kWh)	*CO_2 Emissions* (kg/Year)	*Grid CO_2 Emissions Reduction* (%)	*Grid Energy Cost Reduction* (%)	*Energy Losses* (%)	*Main Renewable Energy Source*	*Energy Storage Capacity Requested*
Grid-PV/WB	100	0.0819	14,888.4	41.78	30.89	0	PV	Higher
Grid-PV/B	100	0.0925	16,916.6	33.85	21.94	0	PV	Higher
Grid-W/B	100	0.3979	13,139.7	48.62	0	0	Wind	Lower
Grid-W	100	0.3251	6430.4	74.85	0	0	Wind	Lower
PV/W/B	100	0.1754	11,439	55.27	0	37.68	PV	Higher
PV/B	100	0.1641	14,892.5	41.76	0	34.52	PV	Higher
W/B	100	0.5385	10,252.6	59.91	0	13.72	Wind	Lower
W	100	1.4515	1621.5	93.66	0	73.74	Wind	Lower
Only grid (ε_G = 1)	100	0.11858	25,572	-	-	-	-	-

5. Conclusions

The aim of this work was to study and compare different options of on/off-grid-connected RESs for electricity supply in Sub-Saharan Africa. The chosen study site was Ngaoundéré, which is located in the northern part of Cameroon, rich in solar and wind energy potential. The main results obtained are presented as follows:

- Grid-connected PV/Wind/Battery was identified as the most cost-effective system for energy supply in this locality;
- The least polluting energy system was the stand-alone Wind-only system;
- Grid-connected HRESs were more economically advantageous than the non-grid-connected HRES;
- Grid-connected RESs could even be economically more profitable than the grid-only system in some cases;
- The renewable energy penetration rate highly influenced the system's electricity cost and the CO_2 emissions. Its increase could either increase or reduce the electricity cost, depending on the used renewable energy resources;
- The CO_2 emissions significantly decreased in the presence of HRES, especially when Wind was the main energy source.
- The parameters that could lead to the improvement of the studied systems costs were: the increase in the project lifetime, the decrease in the discount rate, and the decrease in the battery cost.

Thus, the most economical advantageous system was the Grid-PV/Wind/Battery. It is, however, important to note that this ranking could change in some specific conditions. The stand-alone Wind-only configuration was identified as the environmentally most advantageous studied system.

For rural and remote areas, the stand-alone HRESs are well adapted. Thus, the possibility to reduce the cost of such systems should be explored deeply to make them more competitive. As the energy storage devices are the most costly component in HRES-based battery storage, finding other alternatives of energy storage better than the battery is mandatory. Comparative analysis of different energy-storage-devices-based HRESs will be the focus of our future works.

Author Contributions: Conceptualization, R.Z.F. and E.T.H.; data curation, R.Z.F.; formal analysis, R.Z.F. and E.T.H.; funding acquisition, V.D. and A.S.S.; investigation, R.Z.F. and E.T.H.; methodology, R.Z.F.; project administration, V.D.; resources, V.D.; software, R.Z.F.; supervision, V.D. and S.Y.D.; validation, V.D., A.S.S. and C.B.S.; visualization, R.Z.F.; writing—original draft, R.Z.F., A.S.S., E.T.H. and C.B.S.; writing—review and editing, R.Z.F. and A.S.S. All authors have read and agreed to the published version of the manuscript.

Funding: This research was funded by the Deanship of Scientific Research at King Khalid University for funding this work through the Research Groups Program under grant number (RGP.2/81/43).

Data Availability Statement: Not applicable.

Acknowledgments: The authors extend their appreciation to the Deanship of Scientific Research at King Khalid University for funding this work through the Research Groups Program under grant number (RGP.2/81/43).

Conflicts of Interest: The authors declare no conflict of interest.

Nomenclature

Abbreviations

PV	Photovoltaic
WT	Wind turbine
W	Wind
B	Battery
Batt	Battery
NOCT	Nominal operating cells temperature (°C)
LCOE	Levelized cost of energy
PSDP	Power Supply Deficit Probability
Repl	Replacement cost
Inv	Investment cost
Salv	Salvage value
CRF	Capital Recovery Cost
O$M	Operation and maintenance
invert	Inverter
MPP	Maximum power point
STC	Standard test conditions
ES	Energy system
RE	Renewable energy
min	Minimum
max	Maximum

Symbols

E_G	Annual grid energy supply (kWh)
T_a	Ambient temperature (°C)
G	Solar radiation (kWh/m^2)
G_{ref}	Irradiance at reference condition (kW/m^2)
G_{NOCT}	Solar radiation at NOCT (kWh/m^2)
T_c	Cell temperature (°C or K)
$T_{c,ref}$	Cell temperature at reference condition (25 °C or 298 K)

E_s	Total yearly energy supply (kWh)
E_{s_cons}	Energy supply consumed (kWh)
P_{WT}	Wind turbine output power (kW)
$E_{surplus}$	Surplus total energy supply (kWh)
E_{WT_s}	Wind energy supply (kWh)
V_r	Rated wind speed (m/s)
V_{in}	Cut-in wind speed (m/s)
V_{off}	Cut-off wind speed (m/s)
P_{supply}	Power supply (kW)
P_{demand}	Power demand (kW)
E_{excess}	Annual excess energy supply (kWh)
E_B	Annual energy consumed from Battery (kWh)
x	year variation
Greek symbols	
α	Temperature coefficient (%/°C)
ε_G	Grid availability factor
$\eta_{inverter}$	Inverter efficiency (%)
$	US dollar

Appendix A

Table A1. Pseudo-code of a double-objective firefly optimization [37].

Define the objective functions $y_1(\chi)$, $y_2(\chi)$ where the vector $\chi = (\mu_1, \ldots, \mu_k)$, k is the number of variables
Initialize a population of N_t fireflies χ_a (a = 1, 2, … , N_t)
While *iter* $\leq N_{iter\_max}$ (N_{iter_max} is the maximum number of iterations)
for a = 1:N_t
  for b = 1:N_t ($a \neq b$)
Evaluate the objectives functions based on the operational strategy and satisfying all the constraints
    if $\chi_b^{initial}$ Pareto-dominates $\chi_a^{initial}$
      generate new solution $\chi_a^{updated}$
        if $\chi_a^{updated}$ Pareto-dominates $\chi_a^{initial}$
          $\chi_a^{updated}$ is the new solution in the Firefly population
        else
          $\chi_a^{initial}$ is the new solution in the Firefly population
        end
    end
  end
end
    Sort and find the current best approximation to the Pareto front
    Update *iter*←*iter*+1
end
Results

References

1. Population without Access to Electricity in Sub-Saharan Africa from 2000 to 2021. Available online: https://www.statista.com/statistics/1221698/population-without-access-to-electricity-in-africa/ (accessed on 17 August 2022).
2. Vendoti, S.; Muralidhar, M.; Kiranmayi, R. Techno-economic analysis of off-grid solar/wind/biogas/biomass/fuel cell/battery system for electrification in a cluster of villages by HOMER software. *Environ. Dev. Sustain.* **2021**, *23*, 351–372. [CrossRef]
3. Kumar, P.P.; Saini, R.P. Optimization of an off-grid integrated hybrid renewable energy system with different battery technologies for rural electrification in India. *J. Energy Storage* **2020**, *32*, 101912. [CrossRef]
4. Ramesh, M.; Saini, R.P. Dispatch strategies based performance analysis of a hybrid renewable energy system for a remote rural area in India. *J. Clean. Prod.* **2020**, *259*, 120697. [CrossRef]
5. Singh, S.; Chauhan, P.; Singh, N. Capacity optimization of grid connected solar/fuel cell energy system using hybrid ABC-PSO algorithm. *Int. J. Hydrogen Energy* **2020**, *45*, 10070–10088. [CrossRef]
6. Mahmoudi, S.M.; Maleki, A.; Ochbelagh, D.R. Optimization of a hybrid energy system with/without considering back-up system by a new technique based on fuzzy logic controller. *Energy Convers. Manag.* **2021**, *229*, 113723. [CrossRef]

7. Jahangir, M.H.; Fakourihan, S.; Rad, M.A.V.; Dehghan, H. Feasibility study of on/off grid large-scale PV/WT/WEC hybrid energy system in coastal cities: A case-based research. *Renew. Energy* **2020**, *162*, 2075–2095. [CrossRef]
8. Falama, R.Z.; Ngangoum Welaji, F.; Dadjé, A.; Dumbrava, V.; Djongyang, N.; Salah, C.B.; Doka, S.Y. A Solution to the Problem of Electrical Load Shedding Using Hybrid PV/Battery/Grid-Connected System: The Case of Households' Energy Supply of the Northern Part of Cameroon. *Energies* **2021**, *14*, 2836.
9. Ashtiani, M.N.; Toopshekan, A.; Astaraei, F.R.; Yousefi, H.; Maleki, A. Techno-economic analysis of a grid-connected PV/battery system using the teaching-learning-based optimization algorithm. *Sol. Energy* **2020**, *203*, 69–82. [CrossRef]
10. Cai, W.; Li, X.; Maleki, A.; Pourfayaz, F.; Rosen, M.A.; Nazari, M.A.; Bui, D.T. Optimal sizing and location based on economic parameters for an off-grid application of a hybrid system with photovoltaic, battery and diesel technology. *Energy* **2020**, *201*, 117480. [CrossRef]
11. Teo, Y.L.; Go, Y.I. Techno-economic-environmental analysis of solar/hybrid/storage for vertical farming system: A case study, Malaysian. *Renew. Energy Focus* **2021**, *37*, 50–67. [CrossRef]
12. Zhang, X.; Wei, Q.S.; Soo Oh, B. Cost analysis of off-grid renewable hybrid power generation system on Ui Island, South Korea. *Int. J. Hydrogen Energy* **2022**, *47*, 13199–13212. [CrossRef]
13. Jain, S.; Sawle, Y. Optimization and Comparative Economic Analysis of Standalone and Grid-Connected Hybrid Renewable Energy System for Remote Location. *Front. Energy Res.* **2021**, *9*, 724162. [CrossRef]
14. Thirunavukkarasu, M.; Sawle, Y. A Comparative Study of the Optimal Sizing and Management of Off-Grid Solar/Wind/Diesel and Battery Energy Systems for Remote Areas. *Front. Energy Res.* **2021**, *9*, 752043. [CrossRef]
15. Castillo-Calzadilla, T.; Macarulla, A.M.; Borges, C.E.; Kamara-Estebana, O. A case study comparison between photovoltaic and fossil generation based on direct current hybrid microgrids to power a service building. *J. Clean. Prod.* **2020**, *244*, 118870. [CrossRef]
16. Castillo-Calzadilla, T.; Cuesta, M.A.; Olivares-Rodriguez, C.; Macarulla, A.M.; Legarda, J.; Borges, C.E. Is it feasible a massive deployment of low voltage direct current microgrids renewable-based? A technical and social sight. *Renew. Sustain. Energy Rev.* **2022**, *161*, 112198. [CrossRef]
17. Asamoah, S.S.; Gyamfi, S.; Uba, F.; Mensah, G.S. Comparative assessment of a stand-alone and a grid-connected hybrid system for a community water supply system: A case study of Nankese community in the eastern region of Ghana. *Sci. Afr.* **2022**, *17*, e01331.
18. Muh, E.; Tabet, F. Comparative analysis of hybrid renewable energy systems for off-grid applications in Southern Cameroons. *Renew. Energy* **2019**, *135*, 41–54. [CrossRef]
19. Medina-Santana, A.A.; Cárdenas-Barrón, L.E. Optimal Design of Hybrid Renewable Energy Systems Considering Weather Forecasting Using Recurrent Neural Networks. *Energies* **2022**, *15*, 9045. [CrossRef]
20. Zieba, F.R.; Ngangoum, W.F.; Soulouknga, H.M.; Mbakop, K.F.; Dadjé, A. Optimal Decision-Making on Hybrid Off-Grid Energy Systems for Rural and Remote Areas Electrification in the Northern Cameroon. *J. Electr. Comput. Eng.* **2022**. [CrossRef]
21. Alshammari, N.; Asumadu, J. Optimum unit sizing of hybrid renewable energy system utilizing harmony search, Jaya and particle swarm optimization algorithms. *Sustain. Cities Soc.* **2020**, *60*, 02255. [CrossRef]
22. Sambhi, S.; Sharma, H.; Bhadoria, V.; Kumar, P.; Chaurasia, R.; Chaurasia, G.S.; Fotis, G.; Vita, V.; Ekonomou, L.; Pavlatos, C. Economic Feasibility of a Renewable Integrated Hybrid Power Generation System for a Rural Village of Ladakh. *Energies* **2022**, *15*, 9126. [CrossRef]
23. Agua, O.F.B.; Basilio, R.J.A.; Pabillan, M.E.D.; Castro, M.T.; Blechinger, P.; Ocon, J.D. Decentralized versus Clustered Microgrids: An Energy Systems Study for Reliable Off-Grid Electrification of Small Islands. *Energies* **2020**, *13*, 4454. [CrossRef]
24. Falama, R.Z.; Bakari, H.; Dumbrava, V. Double-objective optimization based firefly algorithm of a stand-alone photovolta-ic/water pumping system for water supply in rural and remote areas: A case study. *J. Electr. Syst. Inf. Technol.* **2021**, *8*, 1–25.
25. Samy, M.M.; Mosaad, M.I.; Barakat, S. Optimal economic study of hybrid PV-wind-fuel cell system integrated to unreliable electric utility using hybrid search optimization technique. *Int. J. Hydrogen Energy* **2021**, *46*, 11217–11231. [CrossRef]
26. Falama, R.Z.; Saidi, A.S.; Soulouknga, M.H.; Salah, C.B. A techno-economic comparative study of renewable energy systems based different storage devices. *Energy* **2023**, *266*, 126411. [CrossRef]
27. Javed, M.S. Performance comparison of heuristic algorithms for optimization of hybrid off-grid renewable energy systems. *Energy* **2020**, *210*, 118599. [CrossRef]
28. Hossain, M.A.; Ahmed, A.; Tito, S.R.; Ahshan, R.; Sakib, T.H.; Nengroo, S.H. Multi-Objective Hybrid Optimization for Optimal Sizing of a Hybrid Renewable Power System for Home Applications. *Energies* **2023**, *16*, 96. [CrossRef]
29. Falama, R.Z.; Menga, F.D.; Hamda Soulouknga, M.; Kwefeu Mbakop, F.; Ben Salah, C. A case study of an optimal detailed analysis of a standalone Photovoltaic/Battery system for electricity supply in rural and remote areas. *Int. Trans. Electr. Energy Syst.* **2022**, *12*, 7132589.
30. Islam, Q.N.U.; Ahmed, A. Optimized controller design for islanded microgrid employing nondominated sorting firefly algorithm. In *Nature-Inspired Computation and Swarm Intelligence*; Academic Press: Cambridge, MA, USA, 2020; pp. 247–272.
31. Chaves-González, J.M.; Vega-Rodríguez, M.A. A multiobjective approach based on the behavior of fireflies to generate reliable DNA sequences for molecular computing. *Appl. Math. Comput.* **2014**, *227*, 291–308. [CrossRef]
32. Where Is Ngaoundere, Cameroon? Available online: https://www.worldatlas.com/af/cm/ad/where-is-ngaoundere.html (accessed on 17 August 2022).

33. European Commission. Photovoltaic Geographical Information System. Available online: https://re.jrc.ec.europa.eu/pvg_tools/fr/#PVP (accessed on 7 February 2021).
34. National Renewable Energy Laboratory (NREL). *The Hybrid Optimization Model for Electric Renewables (HOMER)*; National Renewable Energy Laboratory (NREL): Golden, CO, USA, 2022.
35. Yang, X.S. Firefly Algorithms for Multimodal Optimization. In *International Symposium on Stochastic Algorithms*; Springer: Berlin/Heidelberg, Germany, 2009; pp. 169–178.
36. Yang, X.S. Multiobjective firely algorithm for continuous optimization. *Eng. Comput.* **2013**, *29*, 175–184. [CrossRef]
37. Soulouknga, M.H.; Doka, S.Y.; Revanna, N.; Djongyang, N.; Kofane, T.C. Analysis of wind speed data and wind energy potential in Faya-Largeau, Chad, using Weibull distribution. *Renew. Energy* **2018**, *121*, 1–8. [CrossRef]
38. Rezaei, M.; Khalilpour, K.R.; Mohamed, A.M. Co-production of electricity and hydrogen from wind: A comprehensive scenario-based technoeconomic analysis. *Int. J. Hydrogen Energy* **2021**, *46*, 18242–18256.
39. Shaban, A.H.; Resen, A.K.; Bassil, N. Weibull parameters evaluation by different methods for windmills. *Energy Rep.* **2020**, *6*, 188–199. [CrossRef]
40. Ali, S.A.; Mohammad, F.N.T.; Mohd, R.A.; Mohd, F.M.; Makbul, A.M.R. Feasibility analysis of grid-connected and islanded operation of a solar PV microgrid system: A case study of Iraq. *Energy* **2020**, *191*, 116591.
41. Poly-Crystalline Solar Module/120 Cells/Premium HC Series SEP 290W/295W/300W HC. Available online: https://sunceco.com/sep-290-300w-hc/ (accessed on 16 August 2022).
42. Falama, R.Z.; Kaoutoing, M.D.; Mbakop, F.K.; Dumbrava, V.; Makloufi, S.; Djongyang, N.; Salah, C.B.; Doka, S.Y. A comparative study based on a techno-environmental-economic analysis of some hybrid grid-connected systems operating under electricity blackouts: A case study in Cameroon. *Energy Convers. Manag.* **2022**, *251*, 114935. [CrossRef]
43. Ismail, M.S.; Moghavvemi, M.; Mahli, T.M.I. Design of an optimized photovoltaic and microturbine hybrid power system for a remote small community: Case study of Palestine. *Energy Convers. Manag.* **2013**, *75*, 271–281. [CrossRef]
44. NREL. Life Cycle Greenhouse Gas Emissions from Solar Photovoltaics. 2021. Available online: https://www.nrel.gov/docs/fy13osti/56487.pdf (accessed on 31 May 2021).
45. Raum Energy 3.5. Available online: https://fr.wind-turbine-models.com/turbines/1071-raum-energy-3.5#datasheet (accessed on 16 August 2022).
46. Kaabeche, A.; Diaf, S.; Ibtiouen, R. Firefly-inspired algorithm for optimal sizing of renewable hybrid system considering reliability criteria. *Sol. Energy* **2017**, *155*, 727–738. [CrossRef]
47. Dufo-López, R.; Bernal-Agustín, J.L.; Yusta-Loyo, J.M.; Domínguez-Navarro, J.A.; Ramírez-Rosado, I.J.; Lujano, J.; Aso, I. Multi-objective optimization minimizing cost and life cycle emissions of stand-alone PV–wind–diesel systems with batteries storage. *Appl. Energy* **2011**, *88*, 4033–4041. [CrossRef]
48. Jahangiri, M.; Soulouknga, M.H.; Bardei, F.K.; Shamsabadi, A.A.; Akinlabi, E.T.; Sichilalu, S.M.; Mostafaeipour, A. Techno-econo-environmental optimal operation of grid-wind-solar electricity generation with hydrogen storage system for domestic scale, case study in Chad. *Int. J. Hydrogen Energy* **2019**, *44*, 28613–28628. [CrossRef]
49. Tamba, T.G.; Koffi, F.D.; Monkam, L.; Ngoh, S.K.; Biobiongono, S.N. Carbon dioxide emissions from thermal power plants in Cameroon: A case study in Dibamba Power Development Company. *Low Carbon Econ.* **2013**, *4*, 35. [CrossRef]
50. Kasaeian, A.; Rahdan, P.; Rad, M.A.V.; Yan, W.M. Optimal design and technical analysis of a grid-connected hybrid photovoltaic/diesel/biogas under different economic conditions: A case study. *Energy Convers. Manag.* **2019**, *198*, 111810. [CrossRef]